

# **Zeolite-Templated Carbon Materials for High Pressure Hydrogen Storage**

## **Supporting Information**

Nicholas P. Stadie<sup>\*a</sup>, John J. Vajo<sup>b</sup>, Robert W. Cumberland<sup>b</sup>, Andrew A. Wilson<sup>c</sup>, Channing C. Ahn<sup>a</sup>, and Brent Fultz<sup>a</sup>

<sup>a</sup>California Institute of Technology, 138-78, Pasadena, California 91125, USA

<sup>b</sup>HRL Laboratories, LLC, Malibu, California 90265, USA

<sup>c</sup>Cavendish Laboratory, University of Cambridge, Cambridge CB3 0HE, UK

\*Corresponding author. E-mail address: nstadie@caltech.edu.

## Introduction

Additional materials characterization and data analysis were performed to supplement the results reported in “Zeolite-Templated Carbon Materials for High Pressure Hydrogen Storage” to assure reproducibility of the results, validate the templated structure of ZTCs, further analyze the micropore character of MSC-30 and ZTCs, and to probe differences in chemical bonding between MSC-30 and ZTCs that could clarify their significant difference in skeletal density.

The correlation between BET surface area and excess hydrogen uptake across all temperatures and pressures in ZTCs and the other materials studied is central to the conclusions from this study. In addition to standard hydrogen adsorption/desorption measurements, we also include hydrogen cycling results to show full reversibility of hydrogen uptake and to verify that the experimental error in measurements is acceptable. Secondly, the BET method for characterizing the surface area of materials was supplemented by the Dubinin- Radushkevich method for determining microporous volume to determine the correlation between this value and excess hydrogen uptake at room temperature.

Additional comparison of material properties of ZTC-3 and other ZTCs is important for validating the comparison of our high pressure results to those in the literature. Electron microscopy, both scanning (SEM) and transmission (TEM), was performed to show the similarity of ZTC-3 to “PFA-P7-H” synthesized by Ma et al.<sup>38</sup>, an approximately equivalent reference material to “P7(2)-H” of Nishihara et al.<sup>16</sup>

Finally, some measurements were performed to determine if there were differences in  $sp^2$  or  $sp^3$  chemical bonding in ZTC-3 and MSC-30, including x-ray photoelectron spectroscopy (XPS), electron energy-loss spectroscopy (EELS), and solid-state  $^{13}C$  nuclear magnetic resonance (NMR). The motivation for this additional work was elucidation of the nature of the different skeletal density between the two materials. However, no significant differences were detected that could account for the large difference in skeletal density. The results are consistent with those in the literature, for example by Yang et al.<sup>33</sup> (XPS results) and Ma et al.<sup>32</sup> (NMR results).

## Hydrogen Cycling

Hydrogen uptake isotherms measured up to 30 MPa, using our newly constructed Sieverts apparatus specific to high pressure experiments, were cycled multiple times to ensure repeatability of the results. Hydrogen cycling in all materials studied was achieved without any loss of capacity on adsorption and desorption after many cycles, as expected for pure physisorbent materials. For example, three consecutive hydrogen adsorption/desorption cycles in ZTC-3 at 298 K are shown in Figure S1. The sample was degassed before cycling, as detailed in the Experimental Methods, but was not degassed in between cycles.

## Dubinin- Radushkevich Micropore Volume

Nitrogen adsorption isotherms at 77 K were further analyzed to determine the Dubinin- Radushkevich (DR) micropore volume<sup>21</sup> of each sample. The DR method for treating the  $N_2$  adsorption data was found to be susceptible to similar pitfalls as the BET method, especially for MSC-30 which shows multiple stages of different slopes in the DR curve. However, with consistent treatment of the data for all samples, the hydrogen uptake at 77 K and 298 K is also found to be well approximated by the DR micropore volume in the same way as for BET surface area (shown in Figure S2). The trend is linear, and is  $\sim 5$  mmol excess  $H_2$  uptake per mL of DR micropore volume at 298 K and 30 MPa.

## Electron Microscopy

SEM studies were performed on a Hitachi S-4800 instrument operated at 4.0 keV. Samples were prepared for SEM by dispersing in isopropanol on a holey carbon grid. Evidence can be seen of the superficial likeness between particles of ZTC and the zeolite template from which they were synthesized (shown in Figure S3), similar to that reported by Ma et al.<sup>38</sup>

TEM studies were performed on a FEI Tecnai F20 instrument operated at 200 keV. Samples were prepared for TEM by dispersing a finely ground mixture of ZTC and isopropanol on a holey carbon grid. Low magnification TEM studies were consistent with the SEM data. A high magnification micrograph of a thin region of ZTC-3 is shown in Figure S4, with an inset showing the Fourier transform of the image. The spots in the transformed image confirm the periodicity of the porous structure. The pore to pore spacing of 1.0 nm is consistent with that calculated from DFT treatment of the N<sub>2</sub> adsorption isotherms at 77 K (see Figure 3), and with data reported by Ma et al.<sup>38</sup>

## X-ray Photoelectron Spectroscopy

X-ray photoelectron spectroscopy (XPS) was performed to compare ZTCs to MSC-30, but no appreciable difference was found between them (see Figure S5). XPS studies were performed on a Kratos AXIS Ultra DLD spectrometer with a monochromatic Al-K $\alpha$  source operating at 150 W, with a 20 eV pass energy, and 0.1 eV step (after brief survey spectra were collected). The binding energy was corrected to the most intense peak, which is from sp<sup>2</sup> hybridized carbon, at 285.0 eV. The intensity was not rescaled since identical instrumental conditions were used across all samples. For peak fitting analysis, a Shirley-type background was subtracted and 8 component peaks were fitted, following a previously reported procedure.<sup>33</sup> An example of peak fits is shown in Figure S6. The results are summarized in Table S1, indicating 18% and 19% sp<sup>3</sup> hybridized carbon in ZTC-3 and MSC-30, respectively.

## Electron Energy-Loss Spectroscopy

Electron energy-loss spectroscopy (EELS) was performed to compare ZTCs to MSC-30 and other carbon materials, shown in Figure S7. EELS measurements were performed on a FEI Tecnai F20 instrument operated at 200 keV and equipped with a Gatan Imaging Filter system. To acquire these spectra, the aperture size was 0.6 mm, the dispersion was 0.2 eV pixel<sup>-1</sup>, and the energy shift was 175 eV. Samples were prepared by dispersing a finely ground mixture of sample material and isopropanol on a holey carbon grid. The pre-edge peak was calibrated to 285.0 eV in all samples, a power-law background was subtracted, and the signal intensity was normalized to the same value at high loss. The ratio of the areas of the pre-edge peak to the main carbon 1s edge (>289 eV) was used to determine the relative content of sp<sup>2</sup> and sp<sup>3</sup> hybridized carbon (see Figure S8). This study also shows only a small difference in the amount of sp<sup>2</sup> and sp<sup>3</sup> hybridized carbon between ZTC-3 and MSC-30: approximately 18% and 16% sp<sup>3</sup> content, respectively.

## Solid-State <sup>13</sup>C NMR

Solid-state <sup>13</sup>C nuclear magnetic resonance (NMR) experiments were performed on ZTC-3 and MSC-30 using a Bruker DSX-500 spectrometer equipped with a Bruker 4 mm MAS probe (see Figure S9). The sample spinning rate for MAS experiments was 12 kHz, performed at room temperature under dry

nitrogen gas. The chemical shifts are reported in parts per million (ppm) externally referenced to tetramethylsilane. No significant  $\text{sp}^3$  hybridized carbon in either ZTC-3 or MSC-30 was detected.

### **Acknowledgement**

We thank Carol Garland, Sonjong Hwang, and Joseph Beardslee for assistance with supplementary measurements.

### **Additional References**

38. Ma, Z.; Kyotani, T.; Tomita, A.; *Carbon* **2002**, 40, 2367-2374.

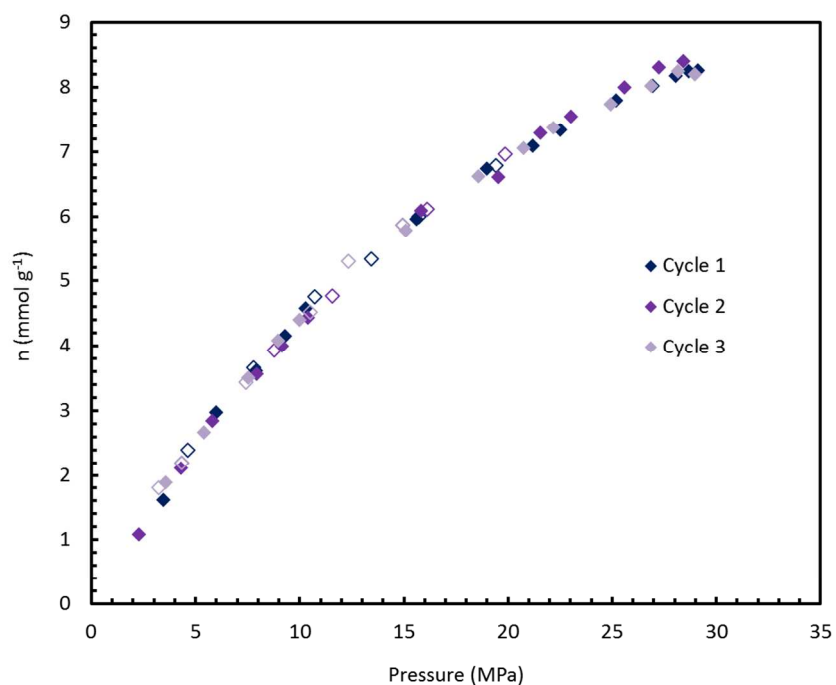


Figure S1. Equilibrium excess hydrogen adsorption/desorption isotherms for ZTC-3 during 3 cycles, showing complete reversibility of hydrogen uptake/delivery which is characteristic of physisorbent materials, and confirming instrument precision.

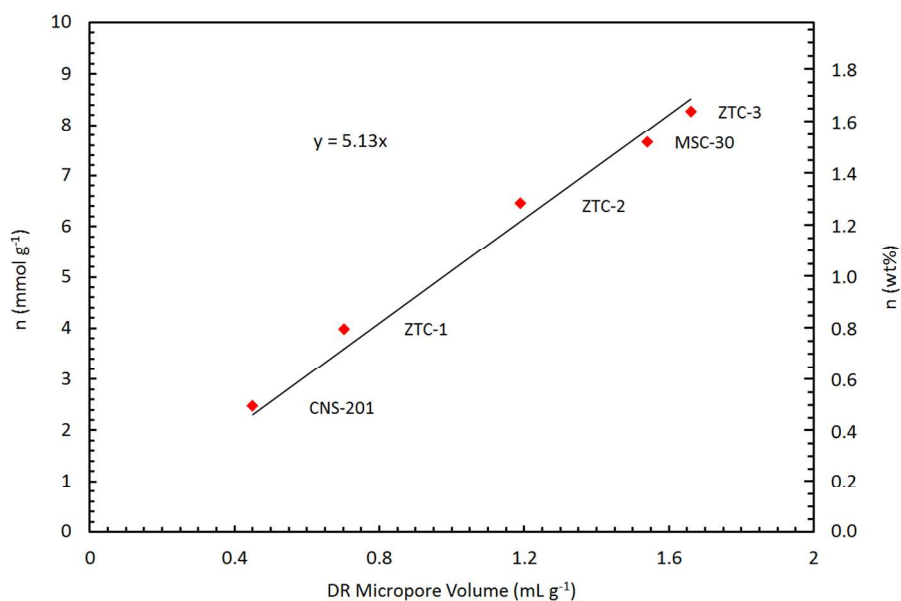


Figure S2. Equilibrium excess adsorption uptake of hydrogen as a function of Dubinin- Radushkevich (DR) micropore volume at 298 K (30 MPa) for all materials studied.

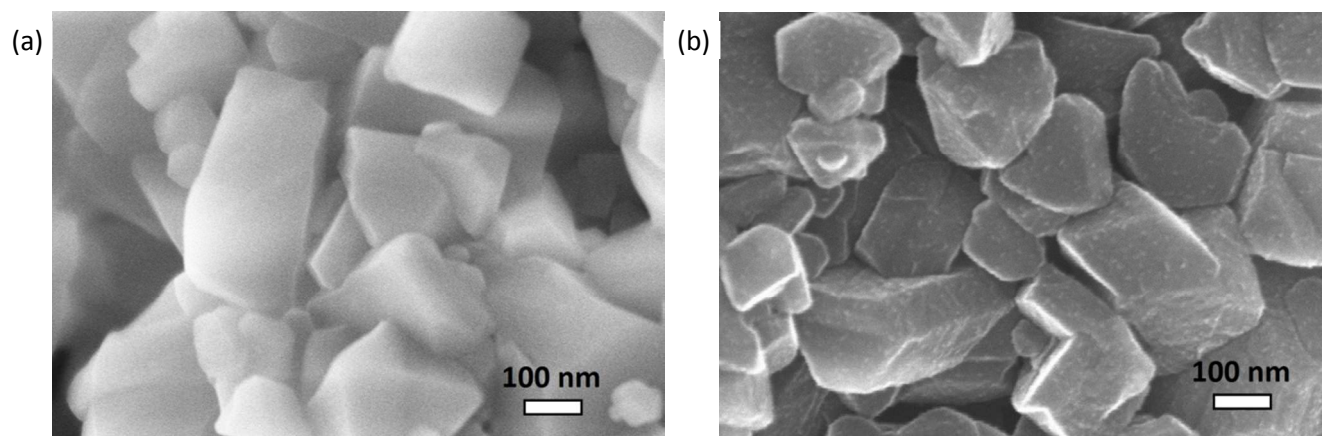


Figure S3. SEM micrographs of zeolite precursor (left) and ZTC product (right), showing similar particle size and shape.

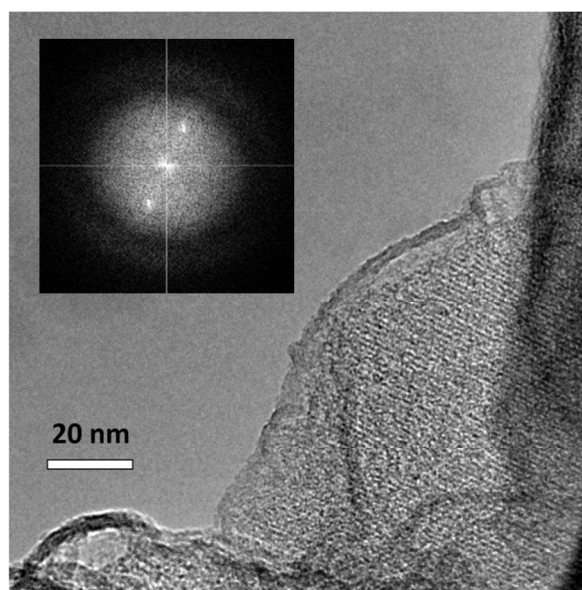


Figure S4. TEM micrograph of ZTC-3 showing pore-to-pore periodicity of 1.0 nm, and the Fourier transform of the image (inset).

Peak Position (eV)	Component Fraction (at%)							
	285.0	285.7	286.4	287.3	288.1	289.4	290.2	291.5
Component	C-C $sp^2$	C-C $sp^3$	C-OR	C-O-C	C=O	O=C-OR	--	--
ZTC-3	53.4	18.0	8.6	6.0	1.1	4.2	1.0	7.7
MSC-30	48.0	18.8	6.8	4.8	6.1	4.2	3.6	7.7

Table S1. Summary of the XPS analysis results for ZTC-3 and MSC-30.

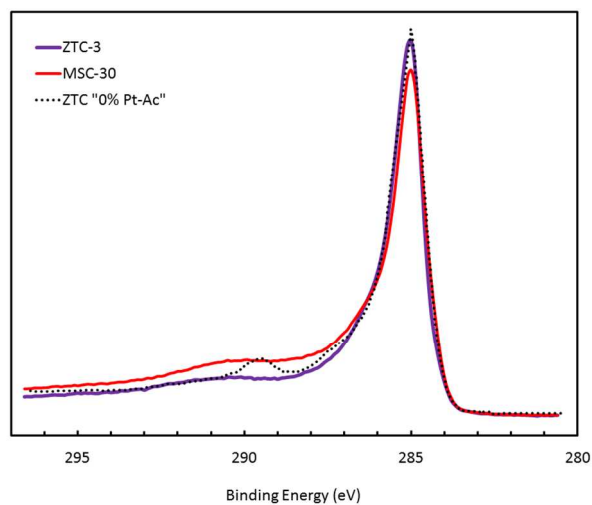


Figure S5. XPS data comparing ZTC-3, MSC-30, and an equivalent reference material, ZTC "0% Pt-Ac."<sup>33</sup>

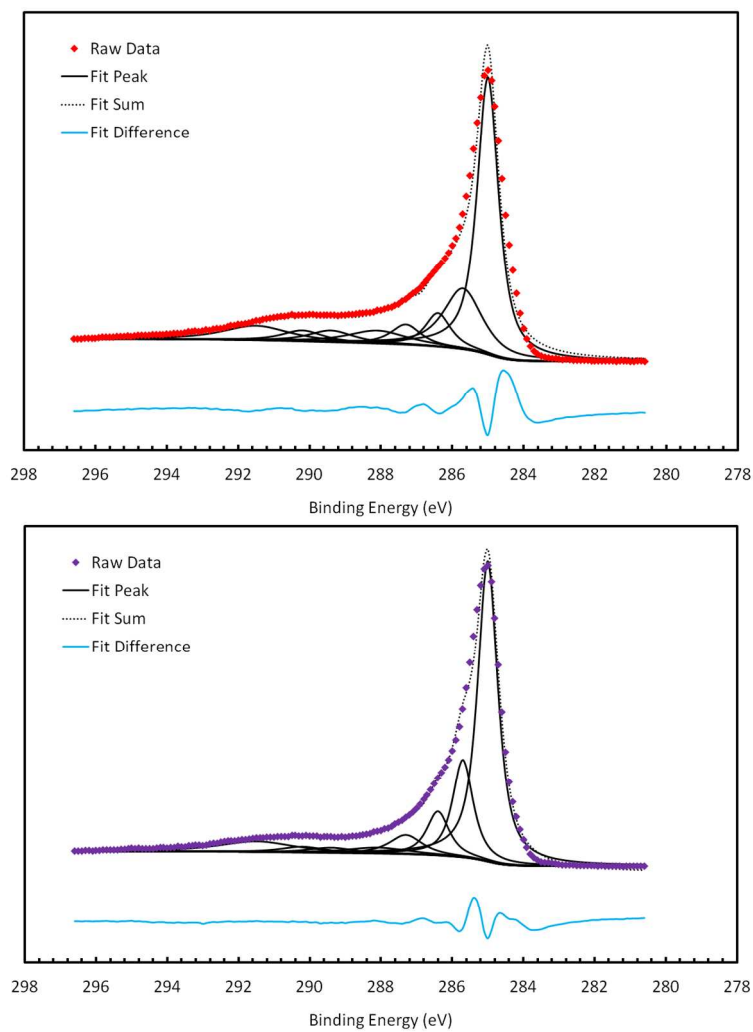


Figure S6. XPS analyses for the carbon 1s regions in MSC-30 (top) and ZTC-3 (bottom).

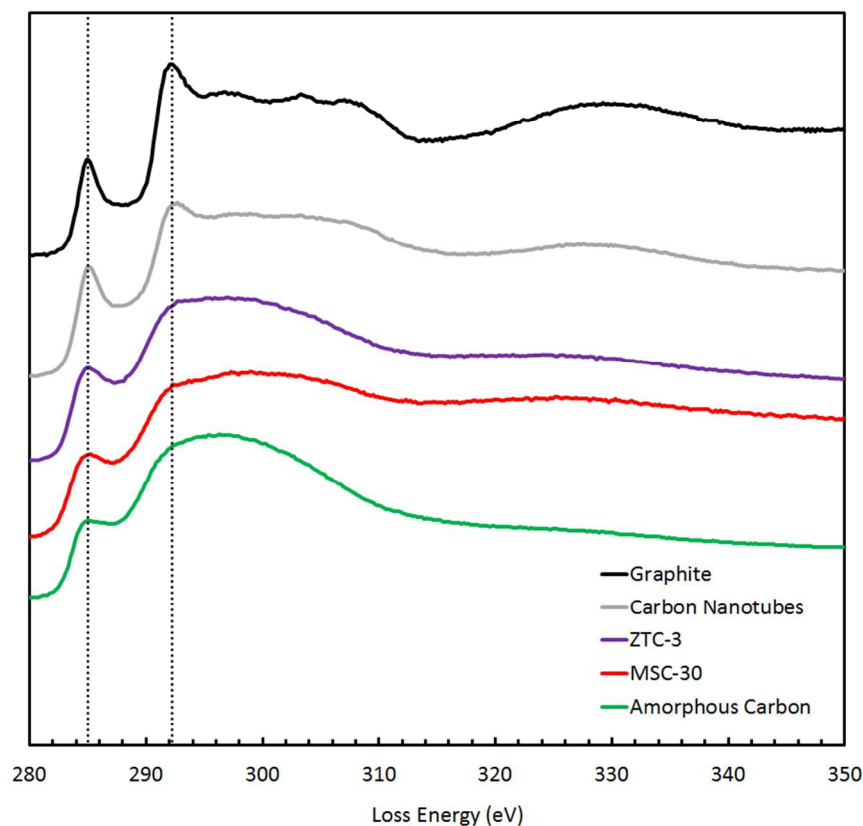


Figure S7. EELS spectra showing the carbon 1s edge in ZTC-3 compared to MSC-30, graphite, carbon nanotubes, and the amorphous holey carbon grid.

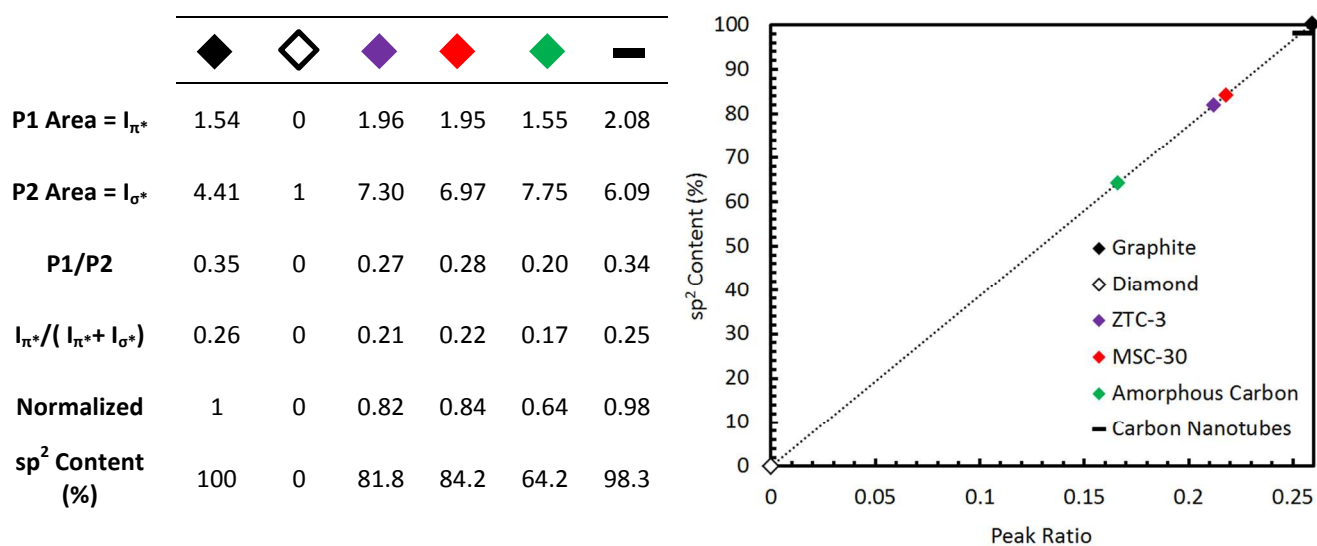


Figure S8. Summary of  $sp^2$  content in carbon materials studied by EELS, based on the integrated peak areas of the  $1s \rightarrow \pi^*$  peak at  $\sim 285$  eV to the  $1s \rightarrow \sigma^*$  peak at  $\sim 292$  eV, and fit to a calibration curve based on graphite and diamond.

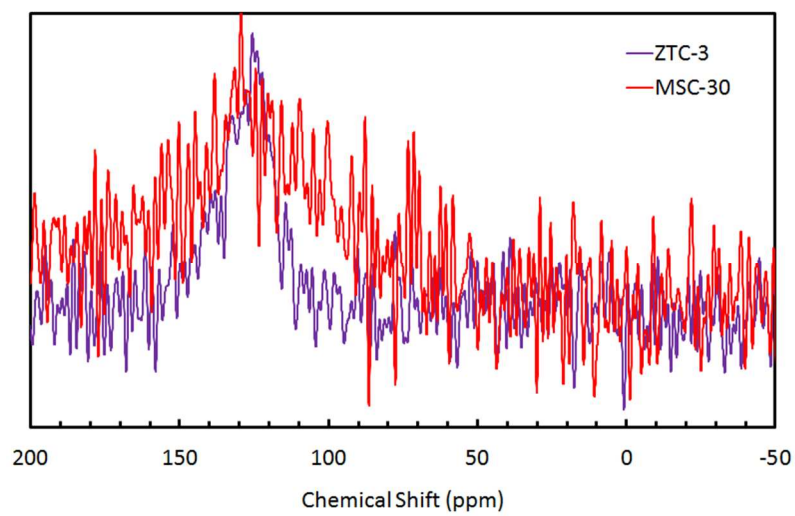


Figure S9. Solid-state  $^{13}\text{C}$  NMR (MAS) spectra of ZTC-3 and MSC-30.